LAWRENCE
LIVERMORE
NATIONAL
LABORATORY

LLNL-JRNL-560792

Effect of n=3 fields below the ELM triggering threshold on edge and SOL transport in NSTX

D. Lore et. al

June 11, 2012

Journal of Nuclear Materials

Disclaimer

This document was prepared as an account of work sponsored by an agency of the United States government. Neither the United States government nor Lawrence Livermore National Security, LLC, nor any of their employees makes any warranty, expressed or implied, or assumes any legal liability or responsibility for the accuracy, completeness, or usefulness of any information, apparatus, product, or process disclosed, or represents that its use would not infringe privately owned rights. Reference herein to any specific commercial product, process, or service by trade name, trademark, manufacturer, or otherwise does not necessarily constitute or imply its endorsement, recommendation, or favoring by the United States government or Lawrence Livermore National Security, LLC. The views and opinions of authors expressed herein do not necessarily state or reflect those of the United States government or Lawrence Livermore National Security, LLC, and shall not be used for advertising or product endorsement purposes.

Effect of n=3 fields below the ELM triggering threshold on edge and SOL transport in NSTX

J.D. Lore*[a], J.M. Canik[a], J-W. Ahn[a], A. Bortolon[b], E.D. Fredrickson[b], M. Jaworski[c], R. Maingi[a], A.G. McLean[d], F. Scotti[c], V. Soukhanovskii[d], and K. Tritz[e]

[a]*Oak Ridge National Laboratory, Oak Ridge, TN 37831, USA*
[b]*University of California-Irvine, Irvine, CA 92697, USA*
[c]*Princeton Plasma Physics Laboratory, Princeton NJ, 08543, USA*
[d]*Lawrence Livermore National Laboratory, Livermore, CA 94550, USA*
[e]*Johns Hopkins University, Baltimore MD, 21287, USA*

Abstract

The pulsed application of n=3 fields below the ELM triggering threshold level results in distinct, transient responses observable on several edge and divertor diagnostics in NSTX. The responses are consistent with increased transport in the plasma edge and scrape-off layer and augmentation of intrinsic strike point splitting due to error fields. These effects are much smaller in magnitude than those of triggered ELMs, and are observed for the duration of the field perturbation measured internal to the vacuum vessel. In addition, changes to the MHD activity are observed, along with regular reductions in the neutron production rate, consistent with the loss of fast beam ions. A characterization of these responses is presented.

PACS: 52.55.Fa, 52.55.Rk, 55.25.Fi

PSI-20 Keywords: Divertor, Edge plasma, ELM control

Corresponding Author Address:

Oak Ridge National Laboratory

1 Bethel Valley Rd

Oak Ridge TN, 37831

Corresponding Author e-mail: lorejd@ornl.gov

Presenting Author: Rajesh Maingi

Presenting Author e-mail: rmaingi@pppl.gov

1. Introduction

The application of small non-axisymmetric magnetic field perturbations has been found to significantly affect edge plasma transport and stability in tokamaks. In NSTX, n=3 applied fields have been used in the paced triggering of edge localized modes (ELMs) [1,2] and the modification of the divertor heat and particle flux profiles [3,4]. Paced ELM triggering allows for control over the secular density rise and impurity accumulation in otherwise ELM-free H-modes. On the other hand, a significant fraction of the plasma stored energy is lost during each ELM, even at the maximum possible triggered ELM frequency. The maximum triggering frequency is limited in the current system by vessel eddy currents as the perturbation coils are external to the vacuum vessel. The divertor heat and particle load during an ELM may become a problem in future devices, or in the planned NSTX-Upgrade. To mitigate or eliminate these deleterious effects, it is important to pursue techniques which may lead to density control and reduced impurity accumulation in plasmas free of large ELMs.

One possible route to such an operating scenario is through the application of n=3 field pulses below the ELM triggering threshold level. This threshold is a function of the applied pulse length and magnitude, as well as the plasma configuration [5]. For pulses near the threshold level, ELMs are triggered only infrequently, however a small transport response is generated during each pulse. A characterization of these responses, measurable on several edge and scrape-off-layer (SOL) diagnostics is presented here.

2. Experimental Setup

In NSTX, 3D field pulses are applied using a midplane coil set normally used for error field correction and resistive wall mode (RWM) feedback control [6]. In the experiments discussed here, these 'RWM coils' have been configured to apply an n=3 field. The coils are external, but close fitting, to the vacuum vessel. Eddy currents induced in the vessel cause the internal field perturbation to lag the coil current waveform. Figure 1a shows the coil current waveform for two different pulse trains: 6ms square pulses (black, solid line) and 3ms square pulses (blue, dot-dashed line). The internal field perturbation is measured by magnetic sensors located ~10cm from the plasma, and peaks at the end of the current pulse (Fig. 1b). The perturbed field amplitude decays over ~10ms. The addition of a

current spike of the opposite sign at the end of the pulse can greatly reduce the decay time (see Fig. 2a).

Several pulse trains that did not result in the regular triggering of ELMs have been investigated. Above a nominal current amplitude, ~1kA, responses are measurable. One case is examined in detail below, with the effect of other pulse duration and amplitudes discussed at the end of section 3a. NSTX Discharge 138146 was configured to have 3ms, 2kA square pulses applied at 40Hz (Fig. 1, dashed blue line). The pulses are used in addition to the n=3 error field correction, but as will be shown in section 3, 'intrinsic' strike point splitting is observed due to error fields. These discharges have lithium wall coatings, with 200mg injected per shot, and are free of ELMs in the absence of 3D fields. The plasmas are near double null, with δ_r^{sep} ~ 5mm, where δ_r^{sep} is the radial distance between the separatricies at the outboard midplane, with high triangularity δ=0.8, and moderate elongation $\varkappa$~2.3. The toroidal field strength B_t=-0.5T, with I_p~800kA, and 4MW of neutral beam power injected.

3. Characterization of responses

The application of non-axisymmetric fields is known to affect both the transport and stability of tokamak plasmas. Generally, even small levels of asymmetry can lead to increased collisional transport, rotation damping, and the creation of magnetic islands and stochastic field regions. In NSTX, the application of n=3 pulses above a threshold level results in robust and controllable triggering of ELMs and modification to the kinetic profiles in the pedestal region [1,2]. The pulses have also been observed to trigger an enhanced confinement regime known as enhanced pedestal H-mode [7]. In addition, 3D fields results alter divertor heat and particle flux profiles through augmentation of the intrinsic strike point splitting and changes in the recycling properties [3,4].

Applying n=3 pulses near the ELM triggering threshold level results in unreliable triggering, as shown in Figure 2. The pulses that do not trigger ELMs nevertheless cause a measurable response in, e.g., the D_α light (Fig. 2b), radiated power (Fig. 2c) and soft x-ray emission from the plasma edge (Fig. 2d), and the neutron production rate (Fig. 2e). The effects can be broadly divided into two categories, changes to the edge, SOL, and divertor transport; and modification of the MHD activity

and the loss of fast ions, followed by a drop in the neutron production rate. The time response of the former is generally proportional to the internal field perturbation, approximately symmetric in time, peaking at internal field maximum. The modification of the MHD activity occurs on a faster timescale, ~0.1ms after the application of the n=3 fields, followed by the reduction in the neutron rate. In both cases the effects are clearly distinct from triggered ELMs, both in magnitude and timescale.

A. Effect on edge, SOL, and divertor transport

Figure 3 shows the D_α emission measured by a) 1D CCD camera and b) a filterscope viewing the divertor. During this time window no ELMs are triggered. Each n=3 pulse results in a ~50% increase in D_α emission and augmentation of the intrinsic strike point splitting. The maximum in the D_α signal occurs at the maximum of the internal field perturbation. Two radial profiles are shown in Figure 4, during the pulse (blue) and between pulses (black). The pulses generally result in a small reduction in the primary peak (R~32cm), with additional peaks observed near R=52 and 61 cm. These effects are consistent with the formation of a topological field structure that occurs from the superposition of the vacuum applied n=3 fields and the axisymmetric equilibrium fields. In this 'vacuum approximation' the axisymmetric separatrix is split into stable and unstable manifolds [5,8], resulting in a 3D field structure where fieldlines followed from within the unperturbed separatrix trace out a series of helical lobes that intersect the divertor plates in a striated pattern [3,9]. Higher fluxes are expected where long connection length fieldlines guide heat and particles from the pedestal region to the divertor. The striated pattern is clearly shown in Figure 5, viewed by a Phantom camera filtered for D_α light [10]. Figure 5 shows the augmentation of the intrinsic splitting directly, the 'background' emission before the n=3 pulse has been subtracted from the emission during the pulse. A similar result is obtained from divertor heat flux measurements from a fast infrared camera, however the camera was configured for a lower triangularity shape and could only view the far SOL for these discharges.

Figure 6 shows the ion saturation current measured by a radial array of triple probes located at the lower divertor (R=63-71cm). The n=3 pulse times are indicated by vertical dashed red lines. At the inner radii, the 'grassy' behavior and the average current (1ms average, orange line), decrease during and immediately following the pulses. At the outer radii the magnitude of the spikes and the average current increases. The unipolar spikes are caused by turbulent transport across the separatrix, and the

different behavior as a function of radius suggests that the n=3 pulses are affecting the turbulence properties. The modulation in the average current versus radius is consistent with helical striations in the divertor particle flux. The radial location of the probes is indicated by vertical dashed lines in Figure 4, however the changes to the profile cannot be directly compared as the diagnostics are located at different toroidal angles and the D_α emission is not directly proportional to the particle flux.

Regular perturbations are also observed several chords of an ultrasoft x-ray (USXR) imaging system viewing in a poloidal array and a bolometer array viewing toroidally along the midplane. The outermost USXR signal is shown in Fig 2d, and an edge bolometer chord in Fig. 2c (for shot 133832, however similar results are obtained for 138146). The effects are localized to the outer chords of both systems ($\psi_N > 0.5$, where $\psi_N=(\psi(R,Z)-\psi_{axis})/(\psi_{sep}-\psi_{axis})$ is evaluated at the point of tangency). There are some indications of an inversion layer at the outer two USXR chords (ψ_N=0.83 and 0.72), however this effect will be studied in more detail using a high resolution system planned for NSTX-Upgrade. While the radiated power in several edge chords shows regular modulations correlated with the n=3 pulses, no significant impact in the total volume integrated radiated power is observed.

The effects described above are also observed for RWM coil square pulses of different duration and amplitude. The responses are scale directly with the internal field perturbation; peaking at the maximum of the field perturbation (end of the square pulse) with a magnitude scaling with the field amplitude. If the pulse length or amplitude is increased beyond the threshold level, an ELM is destabilized.

B. Effects on Fast Ion Population

As the neutron production in NSTX is mostly due to beam target reactions, the 5% drops in the neutron rate observed during the RWM pulses suggest that the magnetic perturbation affects the fast ion transport. This is also indicated by the response of the activity in the MHD modes in the 500-1000kHz range of frequencies, thought to be Compressional and/or Global Alfven Eigenmodes [XX]. These are plasma modes, destabilized through resonance with beam ions. The observed modification of the busting frequency and mode amplitude suggest a modification of the fast ion drive.

RWM fields can affect fast ion confinement through 1) modification of the background kinetic profiles and consequently beam ion birth profile; 2) perturbation of the fast-ion orbits. The latter has

been addressed using the full-orbit Monte Carlo code SPIRAL [XX], including vacuum fields only as zeroth order approximation. Preliminary results indicate a 2% increase of the first orbit losses consistent with the observed reduction of neutron rate. The calculation provides an upper estimate for average heat flux to the plasma facing components associated with these losses of the order of 5 kW/m^2.

4. Comparison to triggered ELMs

The responses discussed in section 3 are distinct from those from triggered ELMs. As shown in Figure 2, the n=3 response precedes the ELM by several milliseconds. The n=3 responses are generally symmetric in time, while the D_α and USXR responses to a triggered ELM have a fast onset and slow decay. The magnitude of the change in the D_α, P_{rad}, and USXR signals is larger during a triggered ELM. In addition, the effects are observed in each USXR and bolometer chord, not localized to the outer channels. Triggered ELMs generally result in measurable changes in global quantities, such as electron and carbon density, kinetic stored energy, and total radiated power. In addition, the triggered ELM response appears to be superimposed over the responses described in section 3a, e.g., the increases in the D_α and USXR signals occur before the ELM is triggered. The fast ion effects described in section 3b are independent of the triggered ELMs.

5. Discussion and Summary

3D pulses below the ELM triggering threshold result in regular, distinct responses measurable by several edge, SOL, and divertor diagnostics. These responses are consistent with increases in the edge transport, e.g., increases in D_α and USXR emission and increased ion saturation current measured by divertor probes. The flux patterns to the divertor are consistent with augmentation of the intrinsic strike point splitting, as measured by divertor cameras and probe arrays. Ideally the 3D field pulses would be used to provide density control and prevent impurity accumulation while avoiding the triggering of ELMs. The tested pulse trains, however, did not result in significant changes to the global plasma quantities. While most of the effects are localized to the plasma edge, the n=3 pulses also affect the core plasma through the loss of fast beam ions, indicated by the modulation of high

frequency MHD modes and reduction in the neutron production rate. These effects are currently under investigation using the full-orbit code SPIRAL.

Acknowledgements

This work is supported by U.S. Department of Energy Contract Numbers DE-AC05-00OR22725 and DE-AC02-09CH11466.

Prepared by LLNL under Contract DE-AC52-07NA27344.

References

[1] J.M. Canik et al., Phys. Rev. Lett. 104 (2010) 045001.

[2] J.M. Canik et al., Nucl. Fusion 50 (2010) 064016.

[3] J-W. Ahn et al., Nucl. Fusion 50 (2010) 045010.

[4] J-W. Ahn et al., Phys. Plasmas 18 (2011) 056108.

[5] J.M. Canik et al., Nucl. Fusion 50 (2010) 034012.

[6] S.A. Sabbagh et al., Phys. Rev. Lett. 97 (2006) 045004.

[7] R. Maingi et al., Phys. Rev. Lett 105 (2010) 135004.

[8] T.E. Evans et al., *Chaos, Complexity and Transport: Theory and Applications*, Singapore: World Scientific (2008).

[9] J.D. Lore et al., Nucl. Fusion 52 (2012) 054012.

[10] F. Scotti et al., *Full Toroidal Imaging of Non-axisymmetric Plasma Material Interaction in the National Spherical Torus Experiment Divertor, (Submitted to Rev. Sci. Inst., 2012)*

Figure Captions

Figure 1. a) RWM coil current waveforms and b) internal magnetic measurements.

Figure 2. Unreliable triggering and plasma response to n=3 pulses that do not trigger ELMs.

Figure 3. D_α measurements from a) 1D CCD divertor camera, b) divertor filterscope.

Figure 4. Radial profiles of D_α emission between 3D field pulses (black, t=424ms) and during a pulse (blue, t=428ms). Times correspond to Fig. 3.

Figure 5: Strike point splitting due to n=3 pulse; emission before the pulse has been subtracted.

Figure 6. Divertor particle flux measured by a triple probe array at the lower divertor.

Figure 7. a) RWM coil current, b) neutron rate, and c) spectrogram data.

Figures

Figure 1:

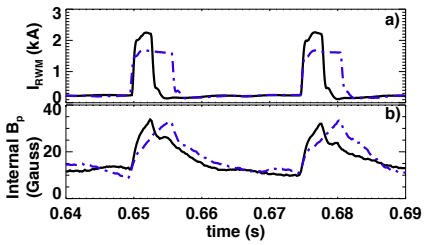

Figure 2:

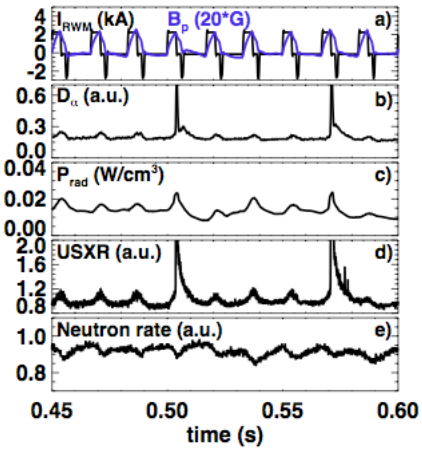

Figure 3:

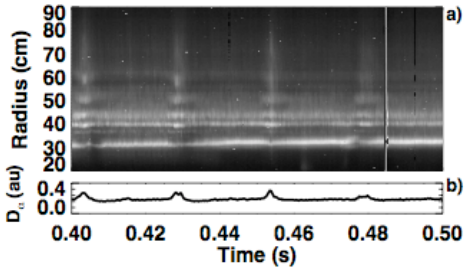

Figure 4:

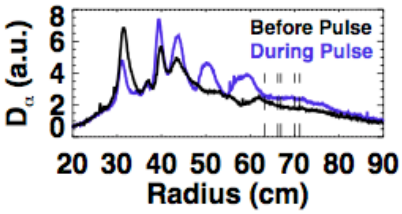

Figure 5:

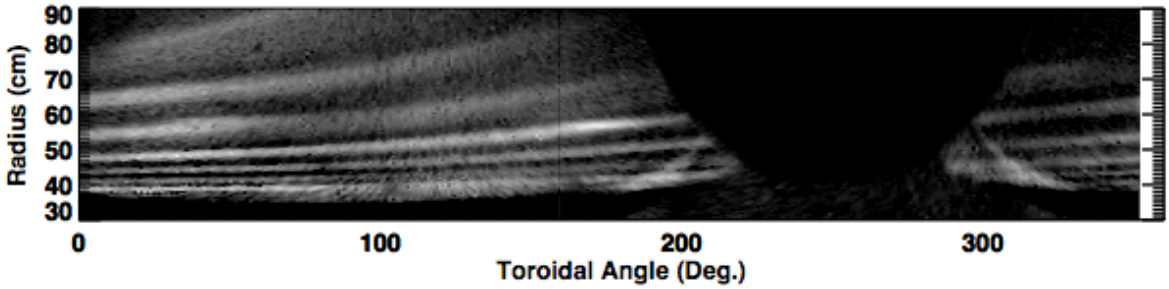

Figure 6:

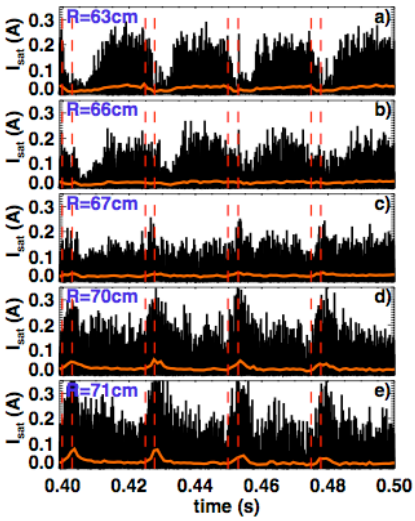
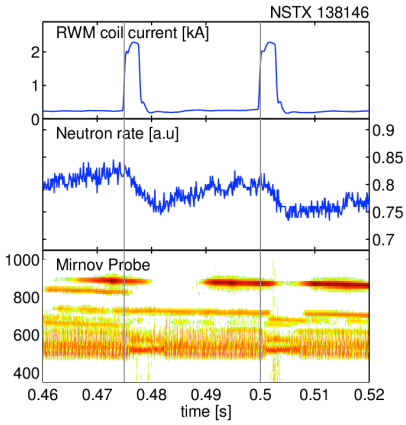
Figure 7: